LA-UR-18-20439
Approved for public release; distribution is unlimited.

Title: Supplement to LA-UR-17-21218: Application to SSVD

Author(s): Tregillis, Ian Lee

Intended for: Report

Issued: 2018-01-22

LA-UR-YY-ZZZZZ

(U) Supplement to LA-UR-17-21218: Application to SSVD

I. L. Tregillis
Plasma Theory and Applications, XCP-6
Los Alamos National Laboratory
Los Alamos, NM 87545

Abstract

We apply the formalism derived in LA-UR-17-21218 [1] to the prescription for an RMI-based self-similar velocity distribution (SSVD) derived by Hammerberg et al. [2]. We compute analytically the true $[m_t(t)]$ and inferred $[m_i(t)]$ ejecta mass arriving at the piezoelectric sensor for several shots described in the literature [3] and compare the results to the data. We find that while the "RMI + SSVD" prescription gives rise to decent estimates for the final accumulated mass at the pin, the time-dependent accumulation rises too sharply and linearly to agree with data. We also compute the time-dependent pressure and voltage at the sensor, and compare the latter to data. The pressure does not rise smoothly from zero, instead exhibiting a strong surge as the leading edge of the ejecta cloud arrives, which produces an initial sharp spike in the voltage trace, which is not observed. These inconsistencies result from a discontinuity in the prescribed self-similar velocity distribution at maximum relative velocity.

1 Relationship between the "RMI + SSVD" formalism and the source AMF, m_c

The RMI-based self-similar velocity distribution (SSVD) prescription derived in [2] provides an expression for the *cumulative* created ejecta mass per unit area in particles with a relative velocity in $[w, \dot{\eta}_s]$ up to creation time t_c:

$$\frac{M(w,t_c)}{A} = m(t_c)\frac{\displaystyle\int_w^{\dot{\eta}_s} g(u)\,\mathrm{d}u}{\displaystyle\int_0^{\dot{\eta}_s} g(u)\,\mathrm{d}u}\,. \tag{1.1}$$

Here $m(t_c)$ is the cumulative mass per unit area as a function of time obtained from the RMI-based ejecta source model,

$$m(t_c) = \frac{2}{3}m_0 \ln\left(1 + \frac{t_c}{\beta'\tau}\right) \tag{1.2}$$

and

$$g(u) \equiv \frac{\xi \mathrm{e}^{-\frac{\xi u}{\dot{\eta}_s}} + 1}{\xi + 1}\,. \tag{1.3}$$

(The authors' convention [2] is that u is the relative velocity, *not* the lab-frame velocity as in [1]). Here we set the spike-tip velocity, $\dot{\eta}_s$, to the final asymptotic value, $\sqrt{3}\eta_{s_0}$, so that it is not time-dependent. A more exact treatment would account for the time-dependence of $\dot{\eta}_s$.

In terms of a source areal mass function (AMF) as defined in [1], the same physical quantity would be expressed as

$$\int_0^{t_c} \mathrm{d}t_c' \int_w^{\dot{\eta}_s} m_c(w', t_c')\,\mathrm{d}w'\,, \tag{1.4}$$

from which it follows that the "RMI + SSVD" prescription provided in [2] yields the following source AMF:

$$m_c(w,t_c) = \frac{\dfrac{\mathrm{d}m}{\mathrm{d}t_c}\cdot g(w)}{\displaystyle\int_0^{\dot{\eta}_s} g(u)\,\mathrm{d}u} \tag{1.5}$$

or

$$m_c(w, t_c) = \frac{2}{3}\, m_0 \cdot \frac{1}{t_c + \beta' \tau} \cdot \frac{\xi \mathrm{e}^{-\frac{\xi w}{\dot{\eta}_s}} + 1}{(2 - \mathrm{e}^{-\xi})\dot{\eta}_s}\,. \tag{1.6}$$

The first factor is the overall normalization of mass per unit area; the second factor is the time dependence (the temporal distribution); and the third factor is the *stationary* velocity distribution function. The velocity distribution is stationary because we have eliminated the time dependence of $\dot{\eta}_s$ by setting it to the final asymptotic value. In a more exact treatment, using some function $\dot{\eta}_s(t)$, the velocity distribution would be non-stationary.

Note the above expression yields the units of an AMF as defined in [1], namely mass per unit volume.

2 True $[m_t(t)]$ and inferred $[m_i(t)]$ accumulated areal mass at sensor

The *true* accumulated mass per unit area at the sensor is the exact analytic solution for a given source AMF, for an ideal system described by the kinematic assumptions baked into the piezoelectric voltage analysis. As demonstrated in [1], the analytic solution is correct regardless of whether the ejecta creation was instantaneous or sustained. It is a direct solution to the kinematics, without any appeal to sensor measurements.

From [1], we have

$$m_t(t) = \int_{\frac{h}{t} - u_{fs}}^{\dot{\eta}_s} \mathrm{d}w \int_0^{t_c(w,t)} m_c(w, t_c')\, \mathrm{d}t_c' \tag{2.1}$$

where

$$t_c(w, t) \equiv \frac{(w + u_{fs})t - h}{w}$$

and, as usual, we have taken the shock breakout time $t_0 = 0$ for convenience, with no loss of generality. Recall that here w is the velocity relative to the free surface and u_{fs} is the free-surface velocity in the laboratory frame. The initial distance from the free surface to the sensor is h. The measurement time is t and the creation time is t_c.

The time integration yields

$$m_t(t) = \frac{2\,m_0\,\xi}{3\,\dot{\eta}_s\,(2-\mathrm{e}^{-\xi})} \int_{\frac{h}{t}-u_{fs}}^{\dot{\eta}_s} \mathrm{e}^{-\frac{\xi w}{\dot{\eta}_s}}\,\ln\left[p(t)+\frac{q(t)}{w}\right]\,\mathrm{d}w + \frac{2\,m_0}{3\,\dot{\eta}_s\,(2-\mathrm{e}^{-\xi})} \int_{\frac{h}{t}-u_{fs}}^{\dot{\eta}_s} \ln\left[p(t)+\frac{q(t)}{w}\right]\,\mathrm{d}w \tag{2.2}$$

where

$$p(t) \equiv 1 + \frac{t}{\beta'\tau} \qquad \text{and} \qquad q(t) \equiv \frac{u_{fs}t - h}{\beta'\tau}\,. \tag{2.3}$$

Both integrals have closed-form solutions. The first integral gives rise to exponential integral functions, which have a branch cut on the negative real axis; however, strict enforcement of causality ensures the physical domain of interest avoids all singularities and branch cuts.

The *inferred* (i.e., measured) accumulated mass per unit area arriving at the sensor is the value that would be obtained through analysis of the piezoelectric voltage signal. The voltage signal is derived from the pressure on the sensor, which is the dynamical ram pressure obtained from the true analytic solution.

From [1], we have

$$m_i(t) = m_t(t) + \frac{1}{h}\int_{\frac{h}{t}-u_{fs}}^{\dot{\eta}_s} w\,\mathrm{d}w \int_0^{t_c(w,t)} t_c'\,m_c(w,t_c')\,\mathrm{d}t_c'. \tag{2.4}$$

After the time integration, the second term becomes

$$\begin{aligned}
&\frac{2\,m_0\,\beta'\,\tau}{3\,\dot{\eta}_s\,h\,(2-\mathrm{e}^{-\xi})} \cdot [p(t)-1] \cdot \int_{\frac{h}{t}-u_{fs}}^{\dot{\eta}_s} \left[\xi\,w\,\mathrm{e}^{-\frac{\xi w}{\dot{\eta}_s}} + w\right]\,\mathrm{d}w \\
&+ \frac{2\,m_0\,\beta'\,\tau}{3\,\dot{\eta}_s\,h\,(2-\mathrm{e}^{-\xi})} \cdot q(t) \cdot \int_{\frac{h}{t}-u_{fs}}^{\dot{\eta}_s} \left[\xi\,\mathrm{e}^{-\frac{\xi w}{\dot{\eta}_s}} + 1\right]\,\mathrm{d}w \\
&- \frac{2\,m_0\,\beta'\,\tau}{3\,\dot{\eta}_s\,h\,(2-\mathrm{e}^{-\xi})} \int_{\frac{h}{t}-u_{fs}}^{\dot{\eta}_s} \ln\left[p(t)+\frac{q(t)}{w}\right]\left[\xi\,w\,\mathrm{e}^{-\frac{\xi w}{\dot{\eta}_s}} + w\right]\,\mathrm{d}w
\end{aligned} \tag{2.5}$$

These integrals have closed-form solutions. As before, the solutions include exponential integral functions, but careful application of causality ensures the physical solution avoids all singularities and branch cuts.

Figure 1 shows $m_t(t)$ and $m_i(t)$ computed for shot 5 of [3]. At the nominal time of free-surface arrival at the sensor ($\frac{h}{u_{fs}} \approx 10.39$ μs), the inferred mass exceeds the true value by just 6.6%.

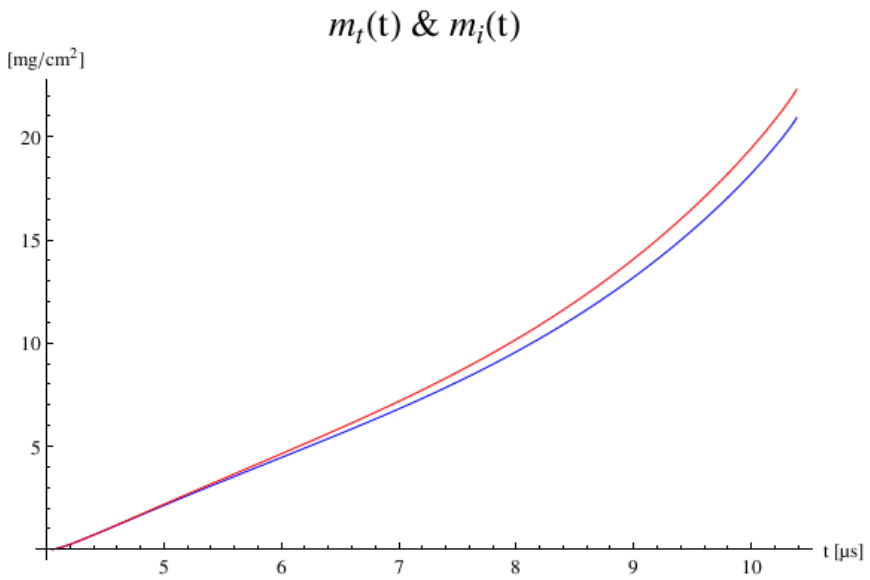

Figure 1: $m_i(t)$ (red) and $m_t(t)$ (blue) computed analytically for Vogan et al., Shot 5.This calculation used $u_{fs} = 1.91$ mm/μs; $\dot{\eta_s} = 2.99$ mm/μs; $h = 19.84$ mm; $m_0 = 4.16$ mg/cm^2; $\beta'\tau = 0.0055$ μs; and $\xi = 7.2$. The published measured value at the time of free surface arrival ($t_{fs} \approx \frac{h}{u_{fs}} = 10.39$ μs) is approximately 16.2 mg/cm^2 ([3], Figure 11); the true and inferred values at this time are 20.9 and 22.3 mg/cm^2, respectively.

Figure 2 shows the same calculations, now plotted as a function of relative velocity, overlaid with the actual measured (inferred) ejecta mass data. We see the analytic calculations, derived from the "RMI + SSVD" prescription, overpredict the mass in high velocities. Note also that the analytically computed masses rise nearly linearly at early times (high velocities), in contrast to the observation.

Results for several shots are compiled in Table 1.

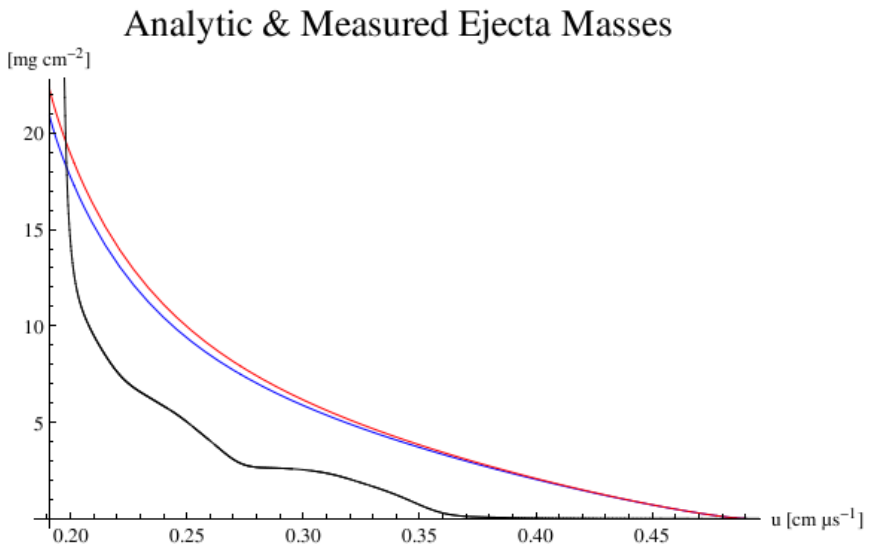

Figure 2: Data (black) overlaid with $m_i(w)$ (red) and $m_t(w)$ (blue) computed analytically for Vogan et al., Shot 5. This calculation used $u_{fs} = 1.91$ mm/μs; $\dot{\eta_s} = 2.99$ mm/μs; $h = 19.84$ mm; $m_0 = 4.16$ mg/cm^2; $\beta'\tau = 0.0055$ μs; and $\xi = 7.2$. The published measured value at the time of free surface arrival ($t_{fs} \approx \frac{h}{u_{fs}} = 10.39$ μs) is approximately 16.2 mg/cm^2 ([3], Figure 11); the true and inferred values at this time are 20.9 and 22.3 mg/cm^2, respectively.

Experiment	kh	Epistemic Uncertainty [%]^a	$m_t(t_{fs})$/published^b
[3] Shot 5	1.5	6.60	1.29
[3] Shot 6	0.19	1.42	2.35
[3] Shot 8	1.27	5.90	1.23
[3] Shot 10	0.08	2.36	1.68
[3] Shot 11	0.22	2.03	1.50
[3] Shot 12	0.25	2.87	1.61

Table 1: Results for six shots from the literature. ^{a}Error imposed by the assumption of instantaneous creation, computed at the time of free surface arrival. ^{b} Ratio of the true analytic accumulated ejecta areal mass computed at the nominal time of free-surface arrival, to the published value.

For these shots, the epistemic uncertainty imposed by the assumption of instantaneous creation *when the source AMF is derived from the specific prescription given in [2]* is less than 7%. The analytically computed final ejecta mass values exceed the measured values by approximately 23-70%, but by 135% in one case.

3 Comparison of instantaneous and self-similar velocity distributions

A measurement of accumulated mass per unit area on the sensor (via analysis of piezoelectric voltages), $\tilde{m}(t)$, implies an AMF at the sensor, $\tilde{m_a}(u,t)$ such that

$$\tilde{m}(t) = \int_0^t \mathrm{d}t' \int_0^\infty \tilde{m_a}(u,t)\mathrm{d}u. \tag{3.1}$$

If the corresponding *source* AMF is assumed to be impulsive, then $\tilde{m_c}(w,t_c) = m_0 f(w)\delta(t_c)$ and

$$f(w) = \frac{h}{m_0 u^2} \left.\frac{\mathrm{d}\tilde{m}}{\mathrm{d}t}\right|_{t=\frac{h}{u}} \tag{3.2}$$

is the ejecta velocity distribution required to produce $\tilde{m}(t)$.

When we have a known source AMF (in this case provided by the "RMI + SSVD" prescription), then we may compare two different velocity distribution functions: the distribution imposed by the source function itself, and the distribution *implied* by the piezoelectric voltage analysis through the assumption of instantaneous creation.

Figure 3 overlays the velocity distribution from Eq. 1.6 and the instantaneously created velocity distribution implied by $m_i(t)$, for Shot 5 of [3]. A large normalization factor was applied to the SSVD to aid comparison.

We see that compared to the instantaneously created velocity distribution (which is guaranteed to reproduce $m_i(t)$ in the case of impulsive ejecta creation), the self-similar velocity distribution overpredicts fast particles and underpredicts slow particles. Furthermore, we see the self-similar distribution does not go smoothly to zero at the maximum relative particle velocity. This has consequences for the time-dependent pressure and voltage, as shown below.

4 Sensor pressure and voltage

As shown in [1], the time-dependent pressure on the sensor, arising from the dynamical ram pressure of the impinging ejecta cloud, can be calculated from the sensor

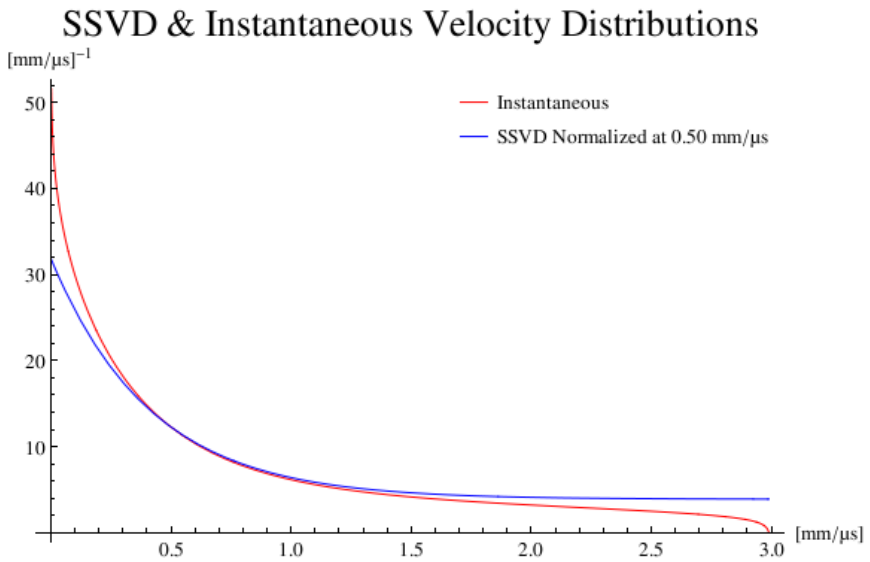

Figure 3: Red: implied (instantaneous) ejecta particle velocity distribution required to match the inferred (measured) cumulative mass at the sensor. Blue: self-similar (time-dependent) velocity distribution, normalized to match the former at $w = 0.5$ mm/μs.. These results were computed for shot 5 of [3].

AMF:

$$P(t) = \int_0^\infty m_a(u,t)\, u\, \mathrm{d}u = \int_{\frac{h}{t}}^{\dot{\eta}_s} \left(\frac{u^2}{u-u_{fs}}\right) m_c \left[u - u_{fs}, \frac{ut-h}{u-u_{fs}}\right] \mathrm{d}u \qquad (4.1)$$

where the second expression comes from applying the mass-conservation relationship between the source (m_c) and sensor (m_a) areal mass functions [1]. The upper limit of integration is the maximum lab-frame ejecta velocity; the lower limit comes from enforcing the causality condition that the measurement time t be equal to or greater than the earliest possible arrival time for particles of lab-frame velocity u.

When the source AMF is obtained from the SSVD prescription, as above, this becomes

$$\begin{aligned} P(t) = {} & \frac{2\, m_0\, \xi\, \mathrm{e}^{\frac{\xi u_{fs}}{\dot{\eta}_s}}}{3\, \dot{\eta}_s\, (2 - \mathrm{e}^{-\xi})} \int_{\frac{h}{t}}^{\dot{\eta}_s + u_{fs}} \frac{u^2 \mathrm{e}^{-\frac{\xi u}{\dot{\eta}_s}}}{ut - h + \beta' \tau (u - u_{fs})}\, \mathrm{d}u \\ & + \frac{2\, m_0}{3\, \dot{\eta}_s\, (2 - \mathrm{e}^{-\xi})} \int_{\frac{h}{t}}^{\dot{\eta}_s + u_{fs}} \frac{u^2}{ut - h + \beta' \tau (u - u_{fs})}\, \mathrm{d}u\,. \end{aligned} \qquad (4.2)$$

The result computed for shot 5 of [3] is shown in Figure 4. Note that LN piezo pins are expected to fail at pressures exceeding 7 kbar [3]; this calculation indicates the sensor pressure never approaches that limit, except in the final instants prior to free-surface arrival.

The strong pressure "surge" at the time of first ejecta arrival (i.e., when the fastest particles arrive) results from the discontinuity in the self-similar velocity distribution at $w = \dot{\eta}_s$. Rather than rising gradually from zero as a tenuous high-velocity tail arrives at the sensor, the momentum flux jumps almost instantaneously as the full flat leading edge of the ejecta cloud impacts the piezoelectric sensor.

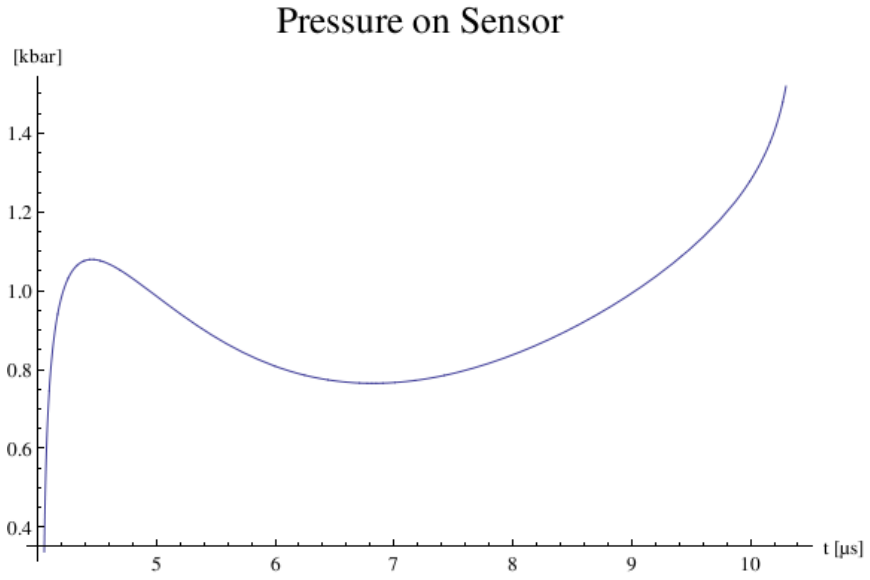

Figure 4: Pressure on the sensor, computed analytically for Vogan et al., Shot 5. This calculation used $u_{fs} = 1.91$ mm/μs; $\dot{\eta}_s = 2.99$ mm/μs; $h = 19.84$ mm; $m_0 = 4.16$ mg/cm^2; $\beta'\tau = 0.0055$ μs; and $\xi = 7.2$.

Empirical observations suggest the bulk of the ejecta cloud should arrive just prior to the free surface. This is seen when the domain of the sensor pressure extends completely to the estimated free-surface arrival time, $t_{fs} \approx \frac{h}{u_{fs}}$, as shown in Figure 5.

Once the pressure on the sensor is known, computing the piezoelectric voltage signal is straightforward:

$$V(t) = A\,R\,S\,\frac{\mathrm{d}P}{\mathrm{d}t} \tag{4.3}$$

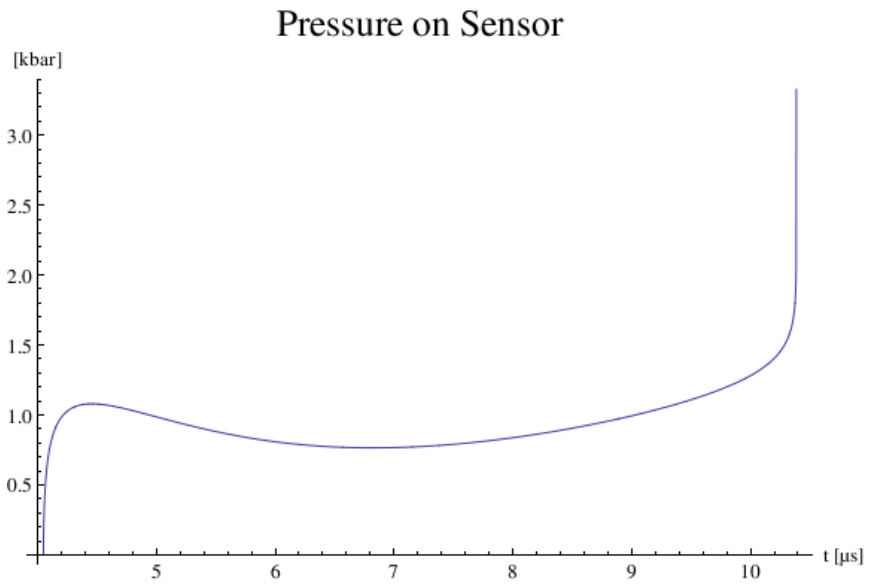

Figure 5: Pressure on the sensor, computed analytically for Vogan et al., Shot 5. This calculation used $u_{fs} = 1.91$ mm/μs; $\dot{\eta}_s = 2.99$ mm/μs; $h = 19.84$ mm; $m_0 = 4.16$ mg/cm^2; $\beta'\tau = 0.0055$ μs; and $\xi = 7.2$. The surge at the time of first ejecta arrival arises from the discontinuity in the velocity distribution at $w = \dot{\eta}_s$.

where A is the collecting area of the piezoelectric sensor, R is the terminating resistance, and S is the piezoelectric sensitivity. The analytically calculated sensor voltage for shot 5 of [3], along with the data, is shown in Figure 6. As expected, the voltage diverges along with the pressure in the limit $t \to t_{fs}$. However, the strong pressure surge at the time of earliest particle arrival means the voltage trace begins with a sharp positive spike, followed by a rapid drop. This is not seen in the data. Between the times of first ejecta arrival and free-surface arrival, the pressure is nearly constant, which keeps the voltage near zero.

5 Pressure and voltage spike mitigation

We may test the assertion that a discontinuity in the self-similar velocity distribution at $w = \dot{\eta}_s$ leads to unphysical spikes in the onset of the sensor pressure and voltage.

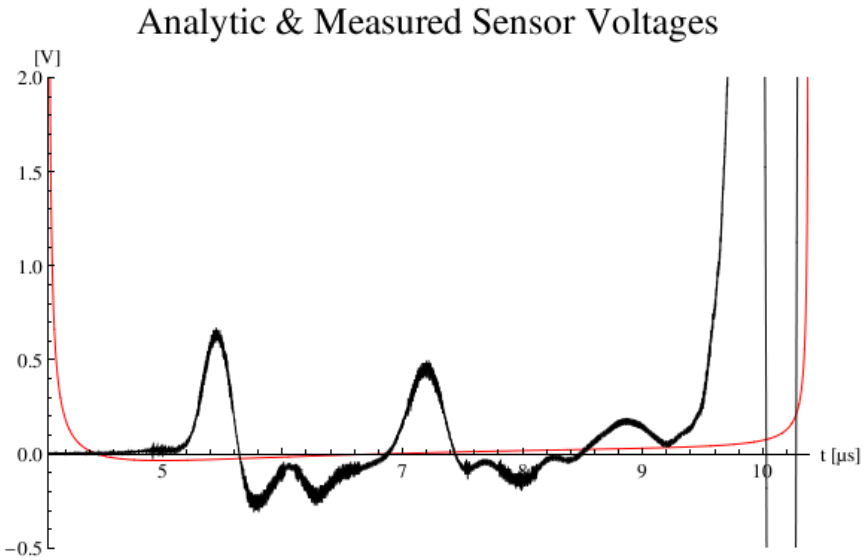

Figure 6: Piezoelectric voltage. Black: data. Red: analytically for Vogan et al., Shot 5. This calculation used $u_{fs} = 1.91$ mm/μs; $\dot{\eta}_s = 2.99$ mm/μs; $h = 19.84$ mm; $m_0 = 4.16$ mg/cm^2; $\beta'\tau = 0.0055$ μs; $\xi = 7.2$; A = 1.267 mm^2; R = 50 Ω; S = 24 pC/N.

To do so, we introduce a linear ramp or "tilt" function:

$$\vartheta(w) = 1 - \frac{w}{\dot{\eta}_s} \tag{5.1}$$

and multiply the velocity distribution by this factor. The original and "tilted" velocity distributions are shown in Figure 7.

The recalculated "tilted" pressure on the sensor is

$$P_{tilt}(t) = \left(1 + \frac{u_{fs}}{\dot{\eta}_s}\right) \cdot P(t) - \frac{2\, m_0\, \xi\, \mathrm{e}^{\frac{\xi u_{fs}}{\dot{\eta}_s}}}{3\, \dot{\eta}_s{}^2\, (2 - \mathrm{e}^{-\xi})} \int_{\frac{h}{t}}^{\dot{\eta}_s + u_{fs}} \frac{u^3 \mathrm{e}^{-\frac{\xi u}{\dot{\eta}_s}}}{ut - h + \beta'\tau(u - u_{fs})}\, \mathrm{d}u$$
$$- \frac{2\, m_0}{3\, \dot{\eta}_s{}^2\, (2 - \mathrm{e}^{-\xi})} \int_{\frac{h}{t}}^{\dot{\eta}_s + u_{fs}} \frac{u^3}{ut - h + \beta'\tau(u - u_{fs})}\, \mathrm{d}u\,. \tag{5.2}$$

The result, and the associated voltage, computed for Shot 5 of [3] are plotted against the original "untilted" calculations in Figures 8 and 9.

We see that gently removing the velocity distribution discontinuity at $w = \dot{\eta}_s$ does mitigate the sharp spikes at the onset of the pressure and voltage on the sensor.

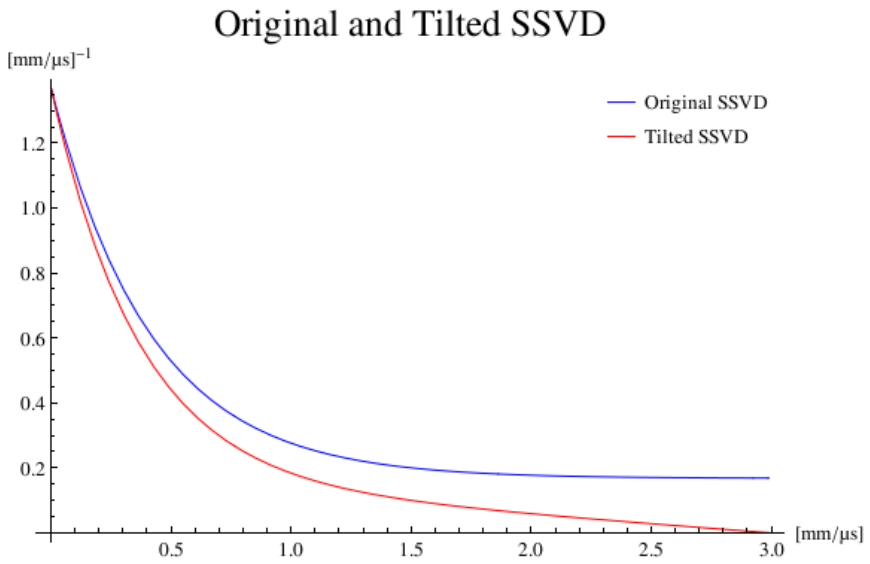

Figure 7: Blue: Original self-similar velocity distribution for shot 5 of [3]. Red: Self-similar velocity distribution modified by the linear ramp $\vartheta(w)$ so that it goes smoothly to 0 at $w = \dot{\eta}_s$.

References

[1] Tregillis, I. L. "(U) An Analytic Study of Piezoelectric Ejecta Mass Measurements," LA-UR-17-21218.

[2] Hammerberg, J. E., Harrison, A. K., Williams, M. W., Margolin, L., Francois, M. M. "(U) A Self-Similarity Velocity Distribution (SSVD) Source Model for Ejecta: Theory, Implementation, and Verification," in process (2017)

[3] Vogan, W. S., Anderson, W. W., Grover, M., Hammerberg, J. E., King, N. S. P., Lamoreaux, S. K., Macrum, G., Morley, K. B., Rigg, P. A., Stevens, G. D., Turley, W. D., Veeser, L. R., and Buttler, W. T. "Piezoelectric characterization of ejecta from shocked tin surfaces," *J. Appl. Phys.* **98**:113508 (2005).

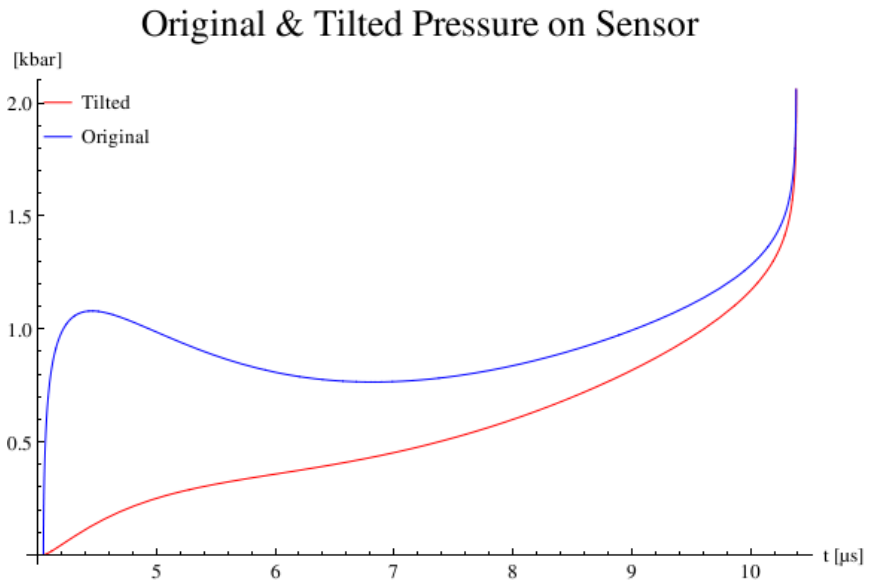

Figure 8: Original (blue) and tilted (red) pressure on the sensor, computed analytically for Vogan et al., Shot 5. This calculation used $u_{fs} = 1.91$ mm/μs; $\dot{\eta_s} = 2.99$ mm/μs; $h = 19.84$ mm; $m_0 = 4.16$ mg/cm^2; $\beta'\tau = 0.0055$ μs; and $\xi = 7.2$.

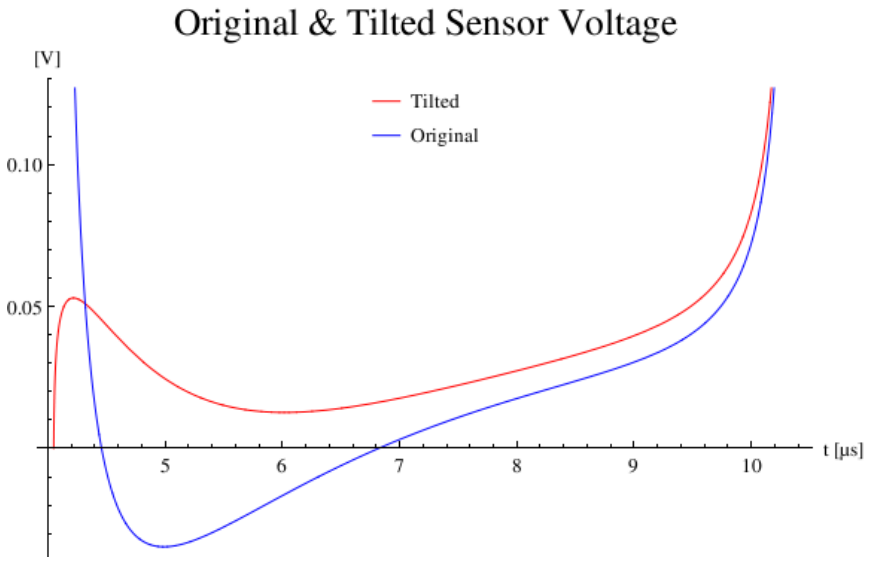

Figure 9: Original (blue) and tilted (red) piezoelectric voltage, computed analytically for Vogan et al., Shot 5. This calculation used $u_{fs} = 1.91$ mm/μs; $\dot{\eta_s} = 2.99$ mm/μs; $h = 19.84$ mm; $m_0 = 4.16$ mg/cm^2; $\beta'\tau = 0.0055$ μs; $\xi = 7.2$; A = 1.267 mm^2; R = 50 Ω; S = 24 pC/N.